

*Phys. Chem. Res.*, Vol. 7, No. 4, 775-783, December 2019  
DOI: 10.22036/pcr.2019.182847.1622

## Effect of Synthesis Temperature on the Electrochemical Properties of Yttrium Aluminum Garnet

V. Mansouri<sup>a,b</sup>, M. Rezaei-Tavirani<sup>a</sup>, M. Rahmandoust<sup>c</sup>, J. Shabani Shayeh<sup>c,\*</sup> and H. Mohammad Shiri<sup>d</sup>

<sup>a</sup>Proteomics Research Center, Shahid Beheshti University of Medical Sciences, Tehran, Iran

<sup>b</sup>Faculty of Paramedical Sciences, Shahid Beheshti University of Medical Sciences, Tehran, Iran

<sup>c</sup>Protein Research Center, Shahid Beheshti University G.C., Tehran, Iran

<sup>d</sup>Department of Chemistry, Payam-e-Noor University, Iran

(Received 23 April 2019, Accepted 8 September 2019)

In this study, yttrium aluminum garnet (YAG) was prepared using a facile electrochemical technique. Four samples were synthesized in 0, 20, 40 and 60 °C by electrochemical pulse deposition and were then calcined at 1200 °C. The effect of synthesis temperature on morphology and structure of YAG was studied using X-ray diffraction, Fourier transform infrared spectroscopy and scanning electron microscopy (SEM) techniques. Furthermore, the electrochemical performance of samples was investigated by cyclic voltammetry and square-wave voltammetry methods. Structural analysis shows that by increasing the synthesis temperature, the network structure of the samples changes from amorphous to the crystalline structure. SEM results also affirm the structural change and show particle size increase in YAG samples from about 90 nm to 2 μm, as a result of rising electrodeposition temperature. The influence of the observed network structure alteration on the catalytic performance of samples was also found to be very significant. Square-wave voltammetry electrochemical analysis of YAG samples leads to enhanced electro-oxidation features, as a result of temperature increase at the synthesis stage. As a proof of concept, the as-prepared YAG samples were successfully employed for electrochemical sensing of ascorbic acid, which showed a significant rise in the electric current of the sensor.

**Keywords:** Yttrium aluminum garnet, Electrosynthesis, Electrochemical performance

### INTRODUCTION

Yttrium aluminum garnet (YAG) ( $Y_3Al_5O_{12}$ ) is a nonmagnetic synthetic optical ceramic material that has many applications in solid-state lasers and acoustic devices [1]. YAG has a body-centered cubic (BCC) crystalline structure, with a band edge of 6.4 to 116 eV, and a theoretical density of 4.5 g cm<sup>-3</sup> [2]. Due to high chemical stability, YAG is generally a good option for high-temperature applications [3,4]. The synthesis method and conditions are, however, very influential on the optical, physical and chemical properties of the fabricated YAG samples [5]. There are different techniques for the synthesis

of YAG, namely sol-gel [6], spray-pyrolysis [7], various solvothermal approaches [8,16,17] and precursor calcination via the thermal treatment of hydroxides in a confined environment [9], from which the last two techniques are capable of synthesizing nanosized YAG. The chemical synthesis routes are, however, mostly time-consuming and require high-temperature synthesis and post-purification steps. Hence, these techniques are generally economically unfavorable. In addition, due to the high band gap, the electrochemical properties of YAG are generally neglected.

Therefore, finding a new fast and low-cost synthesis process that does not require post purification could be very attractive, especially if it leads to improved electric properties as well. According to state-of-the-art reports, electrosynthesis is a fast synthesis technique that needs no

\*Corresponding author. E-mail: [j\\_shabani@sbu.ac.ir](mailto:j_shabani@sbu.ac.ir)

post purification and can effectually improve the electrochemical properties of YAG [10,18]. The YAG nanomaterials produced by one-step, low-temperature electrochemical deposition technique were employed in the structure of poly *ortho*-aminophenol and polypyrrole and caused increased capacitance and stability against continuous cycles [11]. Another feature of the electrochemical synthesis of YAG is an increase in the conductivity of the structure, leading to enhanced composite electrode conductivities [12].

In this work, therefore, YAG was synthesized by cathodic pulse electrochemical deposition at various temperatures and then was heat-treated at 1200 °C, after being detached from the electrode. The electrochemical performances of various YAG samples were studied and compared. The as-prepared YAG samples were finally tested for electrochemical sensing of 0.1 M ascorbic acid.

## EXPERIMENTAL

### Reagents and Materials

All the chemicals used in this study were purchased at analytical grade from Merck Chemical Co., and were used without further purification. Double distilled water was used throughout the experiments.

### Instruments

All electrochemical experiments were carried out using an Autolab General Purpose System PGSTAT30 (Eco-chime, Netherlands). A conventional three-electrode cell with an Ag/AgCl reference electrode was used. Saturated KCl and Pt wire electrodes were employed as the reference and counter electrodes, respectively. The crystallinity of the prepared samples was determined by powder X-ray diffraction (XRD, Phillips PW-1800, Netherlands) using Cu-K $\alpha$  radiation. The samples' morphologies were examined by a scanning electron microscopy (Zeiss (LEO) 1455VP, Germany). Fourier Transform Infrared (FTIR) spectrum was obtained by a Bruker Vector 22 FTIR spectrometer within the range of 400-4000 cm<sup>-1</sup> wave numbers (Bruker Optics, Germany).

All characterization studies were carried out at room temperature. The error bars and standard deviations represent relative signals across three repetitive

experiments.

### Synthesis of YAG Samples

Four YAG samples were electrochemically synthesized as described below: A 316L stainless steel electrode (100 × 50 × 0.5 mm) was placed between two parallel electrodes, namely a graphite electrode (100 × 50 × 0.5 mm) and a saturated calomel electrode, as the counter and the reference electrodes, respectively. After that, the three electrode system was placed in an electrolyte, which contained 5 mM YCl<sub>3</sub>.6H<sub>2</sub>O and 8 mM AlCl<sub>3</sub>.6H<sub>2</sub>O, at a pH of 2.7. By applying a 5 mA pulse current for 20 min, with periods of  $t_{\text{on}} = t_{\text{off}} = 1$  ms, four YAG samples were synthesized over the surface of the steel working electrode, at temperatures of 0 °C (YAG1), 20 °C (YAG2), 40 °C (YAG3) and 60 °C (YAG4). The working electrodes were then washed and dried in room temperature for 36 h. Finally, the samples were detached from the surface of the electrode and were heat-treated at 1200 °C in dry air atmosphere for 2 h.

### Electrode Preparation for Electrochemical Analysis

For electrochemical analysis of the YAG samples, a carbon paste was prepared by adding a mixture of (5:95) weight ratio of YAG samples and graphite powder to double distilled water. Under stirring, the mixture was heated until the water was completely evaporated. The obtained mixture was then mixed by mineral oil, with a ratio of (75:25), and was placed at the bottom of a glass tube with a surface area of 0.07 cm<sup>2</sup>. The electrical connection between the as-prepared electrode and the electrochemical device was implemented using a copper wire fitted into the glass tube. A fresh shiny electrode surface was obtained by smoothing the resulted surface on white paper.

## RESULTS AND DISCUSSION

### Morphology Studies

Figure 1 represents the SEM micrographs of the as-prepared YAG samples, at temperatures of 0 °C (YAG1), 20 °C (YAG2), 40 °C (YAG3) and 60 °C (YAG4). As illustrated, by increasing the synthesis temperature, particle sizes increased from around 90 nm to 2  $\mu$ m. The temperature rise also led to a higher degree of crystallinity

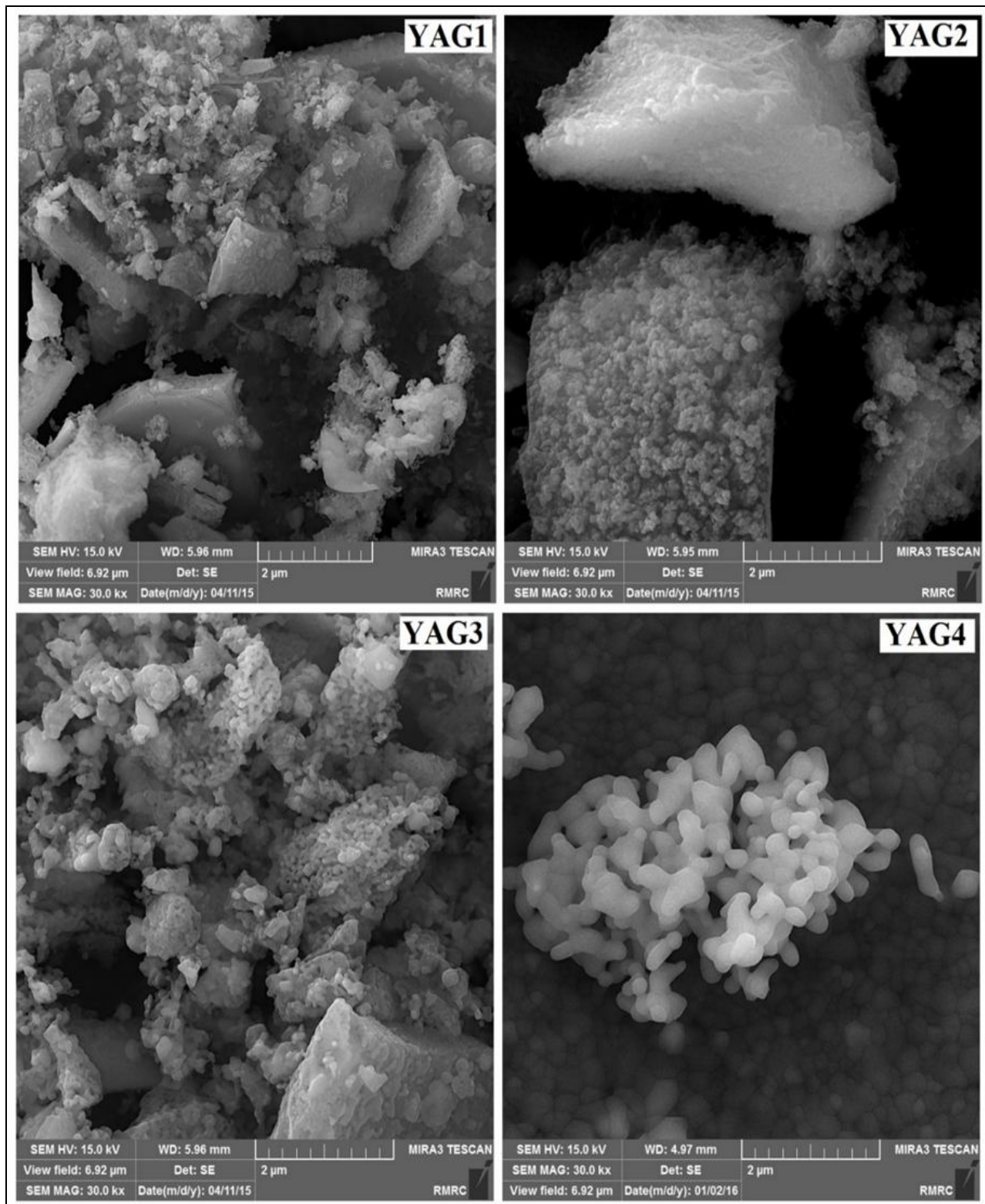
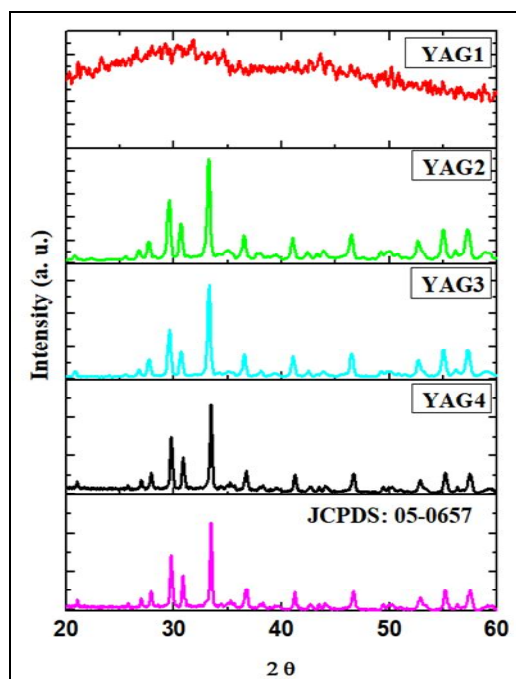


Fig. 1. SEM graphs of the four YAG samples, produced at various temperatures.



**Fig. 2.** XRD diagrams of the as-prepared YAG samples.

**Table 1.** Quantitative Information about the Elemental Content of YAG1 Sample (n = 3)

Element	W.% ( $\pm 3$ )	A%	Error%
O	46.7	67.2	3.5
Al	31.9	27.2	0.9
Y	21.4	5.5	2.6

in YAG particles. These phenomena can be due to the temperature rise leading enhanced kinetic energy of the particles and subsequent easier core growth after nucleation of YAG particle. However, according to state-of-the-art studies, optimization of the thermal treatment is expected to influence the properties of the produced YAG samples as well [9].

### Structural Characterizations

Figure 2a shows the XRD diagrams of the four YAG samples. As illustrated, from YAG1 through YAG4, by

increasing the synthesis temperature, the crystalline structure of samples gets formed. This result is in agreement with the data obtained from the XRD patterns of the samples. It is clear that although the characteristic peak of YAG1 at 29°, attributed to the (222) plane of the cubic yttrium oxide ( $Y_2O_3$ , yttria) phase [9], can be recognized, due to the small size of the formed particles, the peak is significantly superimposed by the amorphous pattern of its environment, making it hard to be distinguished. Therefore, elemental analysis and FTIR were performed to affirm the formation of the YAG particles at 0 °C. Table 1 provides

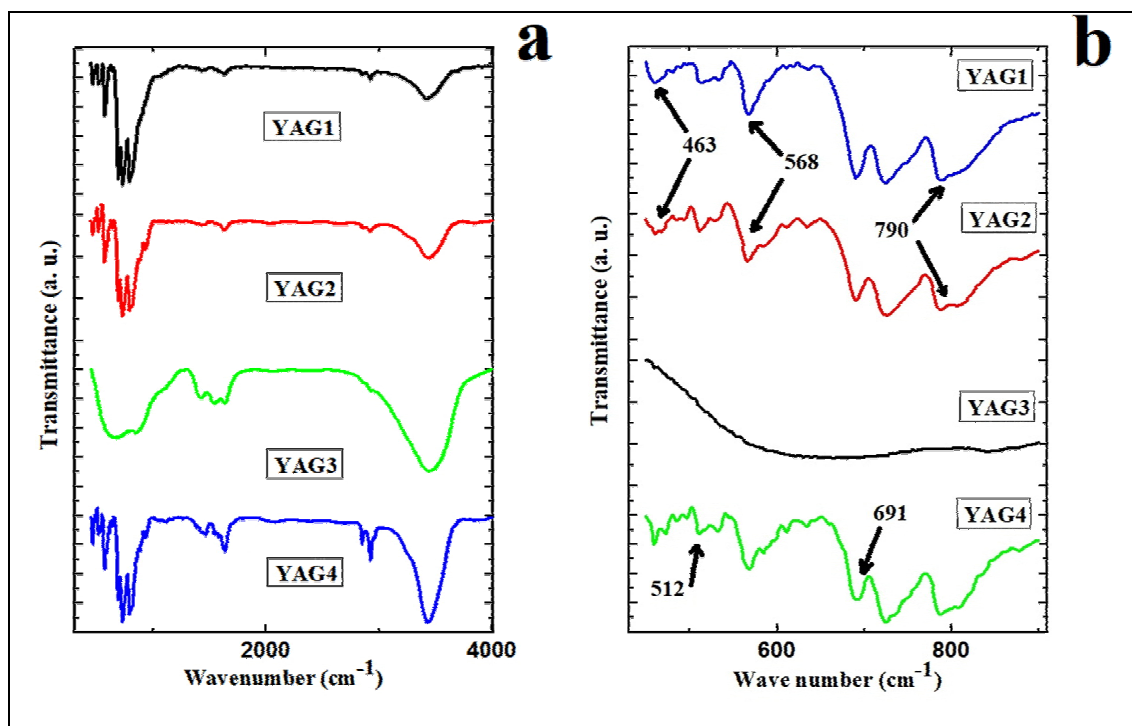


**Fig. 3.** (a) FTIR diagrams for the as-prepared YAG samples, (b) higher resolution of the FTIR in the range below  $1000\text{ cm}^{-1}$ .

quantitative information about the as-prepared YAG samples, showing no impurities. However, increasing the synthesis temperature manifests the samples' crystal structures more significantly. The XRD patterns of YAG2 to YAG4 samples shows a complete crystallization process, where amorphous contributions and possible impurities are no more detected above the baseline. For this very reason, the diffraction peaks get strong and sharp at  $2\theta = 18.19$ ,  $29.74$  and  $33.42$  (see the intensity of the peaks in Fig. 2a) [5].

Figure 3a shows the FTIR spectrum of the YAG samples. As it is seen, there are well-defined peaks at  $790$ ,  $722$ ,  $691$ ,  $568$ ,  $512$ ,  $463\text{ cm}^{-1}$ , as zoomed in Fig. 3b, in the range below  $1000\text{ cm}^{-1}$ , that characterizes the Y-O and Al-O stretching frequencies [2]. One of the notable points, in the study of YAG samples, is the similarity of FTIR spectrum in all samples, showing that the four synthesis procedures yield to successful YAG formation and the differences between the samples are only limited to the extent of their crystallinity and sizes.

### Electrochemical Characterization

Cyclic voltammetry (CV), as a very useful electrochemical technique for evaluating various electrodes [13], was employed in this investigation. Figure 4A represents the CVs of YAG1 electrode in basic, acidic and buffer solution for investigation of its electrochemical nature. It is well-known that the charge transport mechanism in a modified electrode is affected by ionic transfer at the electrode/electrolyte interface [14]. As it shows, in basic and buffer solutions, the YAG1 electrode does not show any charge transfer reactions, whereas, in an acidic solution, two redox peaks appear to describe how electrochemical charge transfer reaction of YAG occurs in the presence of  $\text{H}^+$  ions. The appearance of the two electrochemical redox peaks can be attributed to the interband transitions from the upper valence band of oxygen ( $2p^6$ ) to the conduction bands of yttrium ( $4d + 5s$  states) [2]. As mentioned earlier, the synthesis process of YAG samples critically influences their chemical and electrochemical properties. The effect of the synthesis process on the

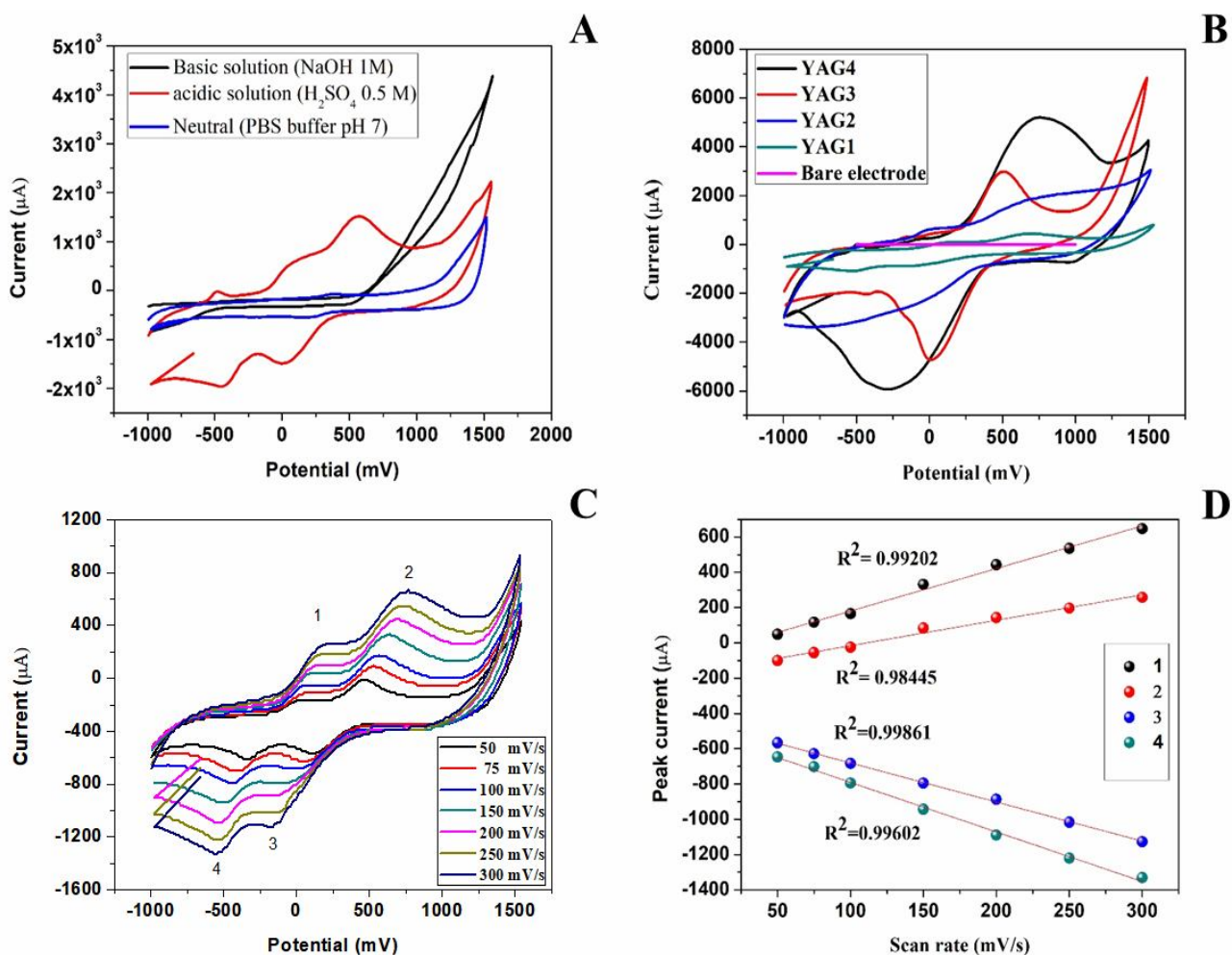


**Fig. 4.** (A) CVs of YAG1 electrode in three solution media, (B) CVs of YAG electrodes at the scan rate of 50 mV s<sup>-1</sup> in 0.5 M H<sub>2</sub>SO<sub>4</sub> solution, (C) CVs of YAG1 electrode in 0.5 M H<sub>2</sub>SO<sub>4</sub> at the various potential sweep rates, and (D) dependency of current peaks of YAG1 electrode as a function of scan rate. The error bars represent relative signals across three replications.

electrochemical nature and performance of the fabricated YAG samples can be observed in Fig. 4B. As it is seen, YAG1 electrode has two small redox peaks getting broader and stronger in YAG2 electrode. Furthermore, in YAG2 electrode, the first anodic peak starts to disappear, which in YAG4 electrode is completely vanished, showing that as expected, by the formation of crystal structure, the electrochemical charge transfer in crystal network gets easier [2,15]. Disappearance of the first redox peak and enhancement of the second one occur as a result of

increasing the synthesis temperature in YAG samples. Figure 4C shows the CVs of YAG1 electrode in 0.5 M H<sub>2</sub>SO<sub>4</sub> at various scan rates. As illustrated, the maximum current for anodic and cathodic half cycles increases by increasing the scan rate. Furthermore, the peak potentials of anodic and cathodic peaks are shifted to the positive and negative potentials, respectively. In the higher ranges of sweep rates, in the YAG1 electrode, the peaks' currents are proportional to the square roots of the sweep rates, highlighting the dominance of the diffusion controlled

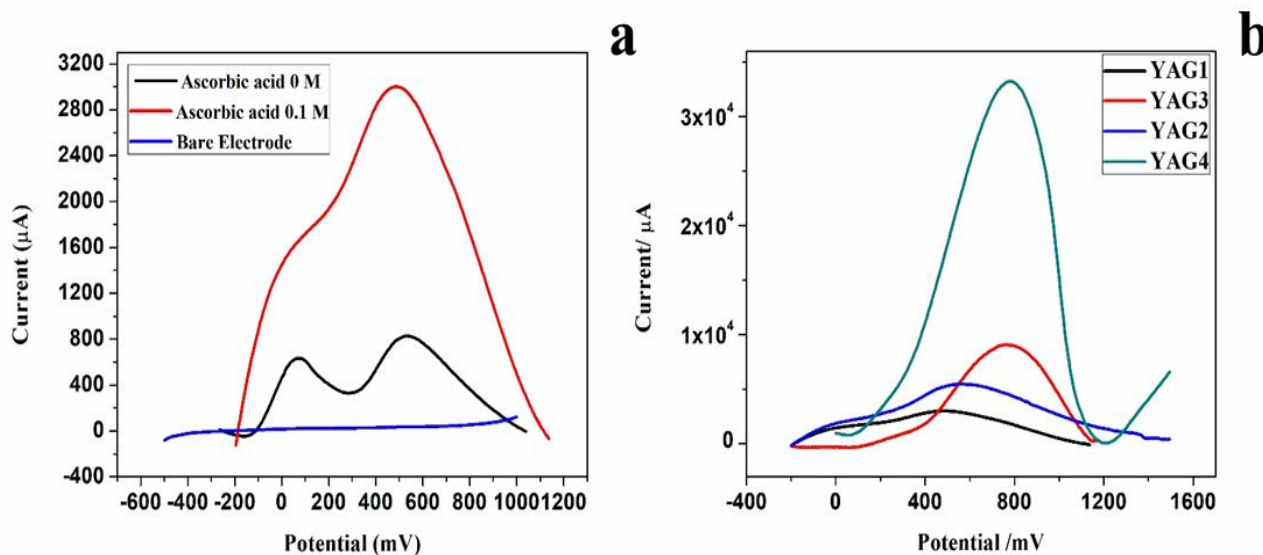


**Fig. 5.** Square-wave voltammograms of (a) YAG1 electrode in 0.5 M H<sub>2</sub>SO<sub>4</sub> solution, containing 0 and 0.1 M ascorbic acid, and (b) all YAG electrodes in 0.5 M H<sub>2</sub>SO<sub>4</sub> solution containing 0.1 M ascorbic acid.

process (Fig. 4D). However, although the dependency of peak currents to the square root of scan rate can be seen, as described earlier for Fig. 4B, the first redox peaks disappear in other electrodes; *i.e.*, YAG2 to YAG4, and the diffusion-controlled reaction is observed by just one redox peak.

As described earlier, increasing the synthesis temperature causes higher kinetic energy of the particles leading to the better core growth and subsequently larger YAG particles. The larger the particles are, the less the amorphous environment is capable of superimposing the crystallinity of the YAG particles. Hence, temperature elevation manifests more evident crystallinity, which in turn causes an enhancement in the redox peak current and improves the electrochemical performance of the samples.

### Electrocatalytic Activity

Electrocatalytic activity of YAG samples is a very important feature, which can be a good representative of the performance of the fabricated materials as a sensor. Figure 5a shows the square-wave voltammograms of the YAG1 electrode in 0.5 M H<sub>2</sub>SO<sub>4</sub> solutions, containing 0 M and 0.1 M ascorbic acid; *i.e.*, in the absence and the presence of ascorbic acid. As illustrated, in the absence of ascorbic acid, two oxidation peaks are observed, similar to the results obtained from the CV technique. Addition of the ascorbic

acid resulted in an increase in both anodic currents, proving a good electrocatalytic activity of the electrode in acidic media for electro-oxidation of biomolecules and organic compounds. Although an increasing trend is observed in both anodic currents, the second peak shows higher electrocatalytic performance. Figure 5b shows the square-wave voltammograms of all YAG electrodes in 0.5 M H<sub>2</sub>SO<sub>4</sub> and 0.1 M ascorbic acid. As it is seen, by adding ascorbic acid, the anodic currents are significantly increased. The magnitude of the current-change increased only four-times in the YAG1 sensor, whereas, in YAG4 sample, the magnitude of the current increased for about two orders of magnitude; *i.e.*, a hundred times more, showing the reliable electrocatalytic activity of the sensors based on the YAG4 sample.

### CONCLUSIONS

Yttrium aluminum garnet has many applications in solid-state lasers and acoustic devices. However, due to the high band gap, the electrochemical properties of YAG are generally neglected. In this study, a simple and low-cost synthesis method was employed that does not require post purification, and more importantly, it is capable of producing a range of YAG particles from nano to micron

size, with effective electrochemical properties. Four YAG samples were prepared using a facile electrochemical pulse deposition technique in 0, 20, 40 and 60 °C and were then calcined at 1200 °C. The effect of synthesis temperature on morphology and structure of YAG was studied using XRD, FTIR and SEM. Furthermore, the electrochemical performances of the samples were investigated by cyclic and square-wave voltammetry methods.

Structural analysis shows that by increasing the synthesis temperature, network structures of the samples change from amorphous to crystalline structure. It is noteworthy, however, that the characteristic (220) peak is observed in the YAG1 sample or the nano-sized YAG, but it is superimposed by the amorphous pattern of the environment. In the other three YAG samples, on the other hand, by size growth, complete crystallization becomes evident. SEM results also affirm the structural changes and show particle size increases in YAG samples from about 90 nm to 2 μm, as a result of increasing the electrodeposition temperature. The influence of the observed network structure alteration on the catalytic performance of samples was also found to be very significant. Square-wave voltammetry electrochemical analysis of YAG samples shows enhanced electro-oxidation features, as a result of elevated synthesis temperature. Based on the good electrocatalytic activity, the YAG electrodes were successfully employed for electrochemical sensing of 0.1 M ascorbic acid, as a proof of concept which resulted in a significant increase in the electric current of the sensor. The as-prepared YAG electrodes are therefore expected to provide the possibility of being employed as good candidates for electrochemical sensing of biomolecules and organic compounds.

## REFERENCES

- [1] Gowda, G., Synthesis of yttrium aluminates by the sol-gel process. *J. Mater. Sci. Lett.*, **1986**, *5*, 1029-1032, DOI: 10.1007/BF01730273.
- [2] Tomiki, T.; Fukudome, F.; Kaminai, M.; Fujisawa, M.; Tanahara, Y.; Futemma, T., Optical spectra of Y<sub>3</sub>Al<sub>5</sub>O<sub>12</sub> (YAG) single crystals in the vacuum ultraviolet region. *J. Phys. Soc. Jpn.*, **1989**, *58*, 1801-1810, DOI: 10.1143/JPSJ.58.1801.
- [3] Manalart, R.; Rahaman, M. N., Sol-gel processing and sintering of yttrium aluminum garnet (YAG) powders. *J. Mater. Sci.*, **1996**, *31*, 3453-3458, DOI: 10.1007/BF00360748.
- [4] Cinibulk, M. K., Synthesis of yttrium aluminum garnet from a mixed-metal citrate precursor. *J. Am. Ceram. Soc.*, **2000**, *83*, 1276-1278, DOI: 10.1111/j.1151-2916.2000.tb01367.x.
- [5] Aghazadeh, M.; Malek Barmi, A. A.; Mohammad Shiri, H.; Sedaghat, S., Cathodic electrodeposition of Y(OH)<sub>3</sub> and Y<sub>2</sub>O<sub>3</sub> nanostructures from chloride bath. Part II: Effect of the bath temperature on the crystal structure, composition and morphology. *Ceram. Int.*, **2013**, *39*, 1045-1055, DOI: <https://doi.org/10.1016/j.ceramint.2012.07.026>.
- [6] Leleckaite, A.; Kareiva, A., Synthesis of garnet structure compounds using aqueous sol-gel processing, *Opt. Mater.*, **2004**, *26*, 123-128, DOI: <https://doi.org/10.1016/j.optmat.2003.11.009>.
- [7] Wang, S.; Xu, Y.; Lu, P.; Xu, C.; Cao, W., Synthesis of yttrium aluminum garnet (YAG) from an ethylenediaminetetraacetic acid precursor. *Mater. Sci. Eng., B*, **2006**, *127*, 203-206, DOI: <https://doi.org/10.1016/j.mseb.2005.10.029>.
- [8] Laishram, K.; Mann, R.; Malhan, N., Single step synthesis of yttrium aluminum garnet (Y<sub>3</sub>Al<sub>5</sub>O<sub>12</sub>) nanopowders by mixed fuel solution combustion approach. *Ceram. Int.*, **2011**, *37*, 3743-3746, DOI: <https://doi.org/10.1016/j.ceramint.2011.05.052>.
- [9] Armetta, F.; Chillura Martino, D. F.; Lombardo, R.; Saladino, M. L.; Berrettoni, M.; Caponetti, E., Synthesis of yttrium aluminum garnet nanoparticles in confined environment, and their characterization. *Colloids. Surf. A*, **2016**, *511*, 82-90, DOI: <https://doi.org/10.1016/j.colsurfa.2016.09.073>.
- [10] Mohammad Shiri, H.; Ehsani, A., Pulse electrosynthesis of novel wormlike gadolinium oxide nanostructure and its nanocomposite with conjugated electroactive polymer as a hybrid and high efficient electrode material for energy storage device, *J. Colloid. Interface. Sci.*, **2016**, *484*, 70-76, DOI: <https://doi.org/10.1016/j.jcis.2016.08.075>.
- [11] Mohammad Shiri, H.; Ehsani, A.; Shabani Shayeh, J., Synthesis and highly efficient supercapacitor behavior



- of a novel poly pyrrole/ceramic oxide nanocomposite film. *RSC Adv.*, **2015**, *5*, 91062-91068, DOI: 10.1039/C5RA19863A.
- [12] Shayeh, J. S.; Ehsani, A.; Naeemy, A.; Shiri, H. M.; Fatemi, F.; Yadegari, A.; Omid, M., Electrosynthesis and characterization of poly aniline/garnet nanoparticles for high-performance electrochemical capacitors, *Ionics*, **2018**, *24*, 505-511, DOI: 10.1007/s11581-017-2217-4.
- [13] Akbari Jonous, Z.; Shayeh, J. S.; Yazdian, F.; Yadegari, A.; Hashemi, M.; Omid, M., An electrochemical biosensor for prostate cancer biomarker detection using graphene oxide-gold nanostructures. *Eng. Life. Sci.*, **2019**, *19*, 206-216, DOI: 10.1002/elsc.201800093.
- [14] Ehsani, A., Influence of counter ions in electrochemical properties and kinetic parameters of poly tyramine electroactive film. *Prog. Org. Coat.*, **2015**, *78*, 133-139, DOI: <https://doi.org/10.1016/j.porgcoat.2014.09.015>.
- [15] Upasani, M.; Butey, B.; Moharil, S. V., Photoluminescence study of rare earth doped yttrium aluminum garnet-YAG:RE (RE: Eu<sup>3+</sup>, Pr<sup>3+</sup> and Tb<sup>3+</sup>). *Optik*, **2016**, *127*, 2004-2006, DOI: <https://doi.org/10.1016/j.ijleo.2015.11.070>.
- [16] Ramanujam, P.; Vaidhyanathan, B.; Binner, J.; Ghanizadeh, S.; Zhou, Z.; Spacie, C., Rapid synthesis of nanocrystalline YAG via microwave-assisted solvothermal process. *J. Am. Ceram Soc.*, **2018**, *101*, 4864-4869, DOI: <https://doi.org/10.1111/jace.15815>.
- [17] Wei, J.; Li, S.; Ren, Y.; Zhang, Y.; Tse, S. D., Investigating the role of solvent formulations in temperature-controlled liquid-fed aerosol flame synthesis of YAG-based nanoparticles. *Proc. Combust. Inst.*, **2019**, *37*, 1193-1201. DOI: <https://doi.org/10.1016/j.proci.2018.07.068>.
- [18] Shabani Shayeh, J.; Ehsani, A.; Naeemy, A.; Shiri, H. M.; Fatemi, F.; Yadegari, A.; Omid, M., Electrosynthesis and characterization of poly aniline/garnet nanoparticles for high-performance electrochemical capacitors. *Ionics*, **2018**, *24*, 505-511. DOI: <https://doi.org/10.1007/s11581-017-2217-4>.